SymFET: A Proposed Symmetric Graphene Tunneling Field Effect Transistor

Pei Zhao[1*], R. M. Feenstra[2], Gong Gu[3] and Debdeep Jena[1]

[1]Department of Electrical Engineering, University of Notre Dame, Notre Dame, IN 46556, USA

[2]Dept. Physics, Carnegie Mellon University, Pittsburgh, PA 15213

[3]Dept. Electrical Engineering and Computer Science, University of Tennessee, Knoxville, TN 37996

Phone: (574)631-1290 Email: *pzhao@nd.edu

Background: Graphene is being considered for alternative channel material for future CMOS technology, due to its high mobility and 2D carrier confinement [1]. The most distinguishing feature of graphene is the symmetric bandstructure, with the valence band a perfect mirror image of the conduction band. The same property carries over to 2D crystals such as Boron Nitride (BN) and less so to Molybdenum disulfide (MoS_2), which can behave as 2D insulators [2]. Attractive devices can be conceived of by stacking 2D crystals and building heterostructures without strain [3]. Experimental work has already demonstrated graphene/insulator/graphene (GIG) heterostructures [3-5]. The proposed BiSFET is based on an excitonic condensate that is a many-body electron-hole state formed in a GIG heterostructure; the power dissipation in computation using the functionality of BISFETs is predicted to be many orders lower than conventional CMOS switching [6]. Recently, we have calculated the tunneling current-voltage curves for finite area GIG heterostructures from a single-particle tunneling viewpoint, more like what happens in TFETs and RTDs. The model predicts a resonant current peak [7], and provides the framework to consider a single-particle tunneling transistor, which we call the "SymFET", since it exploits the intrinsic *symmetry* of the bandstructure of graphene. Here we present the predicted behavior of the SymFET and its characteristics.

Model: We extend the single particle tunneling model described in [7] by adding top and bottom gates that control the quasi-Fermi levels of the top and the bottom graphene layers of the GIG heterostructure. An analytical model is presented to calculate the channel potential and current. The device structure is shown in Figure 1 (a). The current that flows from one graphene layer to the other by tunneling through the insulator. For bias conditions when the two Dirac points are misaligned, only one k-ring in each Dirac cone satisfies the in-plane momentum conservation, and this nonresonant tunneling current is small. When the two Dirac points align, momentum conservation is obeyed for all energies between the left and right quasi-Fermi levels, thus a large resonant current peak is expected (Figure 1 (d)). The detailed expressions for *I-V* curves depending on both the gates and S/D biases are summarized in the left box (T = 0K). Eqs. (1) and (2) are for the nonresonant part of the current, and Eq. (3) is for the resonant part that is summed with Eqs. (1) or (2). The prefactor conductance is $G_1 = \frac{q^2 A}{2\hbar}\left(\frac{\hbar \kappa u_{12}^2 e^{-\kappa t}}{md\, v_F}\right)^2$, κ is a decay constant for the tunneling current in the barrier, L is the coherence length of graphene (size of ordered areas in graphene film), and u_{11} and u_{12} are constants of order unity [7]. ΔE is the separation of quasi-Fermi level and Dirac point, $\Delta E = \Delta E_{doping} + qV_{ch}(V_G, V_D)$ and ΔE_{doping} is the chemical doping. The equations of channel potential $qV_{ch}(V_G, V_D)$ are solved analytically based on the charge neutrality equation, including the quantum capacitance of graphene (some more details are shown in the next page).

$$I = G_1\left(\frac{2\Delta E}{q} - V_{DS}\right), (0 < qV_{DS} < 2\Delta E), (1)$$

$$I = G_1\left(V_{DS} - \frac{2\Delta E}{q}\right), (qV_{DS} > 2\Delta E \text{ or } qV_{DS} < 0), (2)$$

$$I = \frac{1.6}{\sqrt{2\pi}} G_1 \frac{L\Delta E^2 (2u_{11}^4 + u_{12}^4)}{q\hbar v_F} \exp\left\{-\frac{L^2}{4\pi}\left[\frac{(qV_{DS} - 2\Delta E)}{\hbar v_F}\right]^2\right\}, (3)$$

Results and discussions: The expressions given in previous section, is for T = 0K. The room temperature results need to consider the Fermi distribution with integral over energy [7]. The corresponding device parameters are labeled in the figures. A graphene length L = 100 nm is assumed. When the tunnel barrier is thicker, the resonant peak current decreases as expected (Figure 2 (a)). Thinner t_{gate} offers better gate control and higher gate induced doping (and more resonant current). The corresponding resonance peaks increase and shift to higher bias (Figure 2 (b)). Figure 3 explores the entire bias phase space of the *I-V* characteristics. Though the on/off ratio of the SymFET is not a true performance metric, from equation (1) and (3) we find it is given by $I_{on}/I_{off} \approx L\Delta E/\hbar v_F$, (~100 for L ~ 100nm, ~1000 for L ~ 1 μm). It is independent of temperature and increases with size. The I_D-V_{DS} characteristics at fixed V_G are shown in Figure 4(a). In Figure 4(b), the I_D-V_G curve shows strong non-linear behavior. The transconductance can be large in the bias range where the resonant current peak exists. The I_D-V_{DS} curve (e.g. resonant width) is insensitive to the temperature (Figure 5), because of tunneling mechanism, except for Fermi function smearing. The slight difference at low V_{DS}, is due to the Fermi function varying with temperature. The increase of resonant peak current is because Fermi tail extends to high energy with larger density of states. The nonlinear symmetric I_D-V_{DS} behavior can also be used for purposes of frequency multiplication; if a dc voltage bias at the current peak V_{DSp} is superposed with an ac signal, the frequency of the output current will be doubled (Figure 6 schematic). The SymFET is expected to be intrinsically fast since it relies entirely on tunneling; high frequency digital operation and a host of analog applications such as frequency multiplication are thus possible by exploiting the symmetry of the bandstructure of 2D graphene.

978-1-4673-1164-9/12/$31.00 ©2012 IEEE

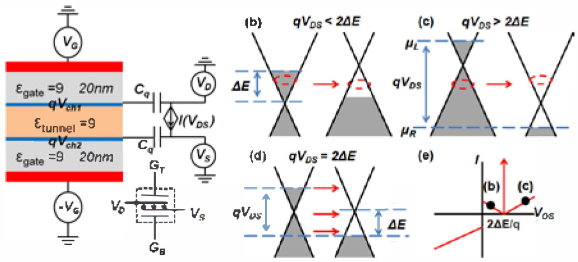

Figure 1: (a) Sketch of the Sym-FET ($V_D = -V_S$). C_q is the quantum capacitance. Insert is the device symbol. The band diagrams for GIG junction at voltages of (b) $qV_{DS} < 2\Delta E$, (c) $qV_{DS} > 2\Delta E$, and (d) $qV_{DS} = 2\Delta E$. When two Dirac points misalign with each other, only one k-ring meets the momentum conservation and current is small. When Dirac points align together, carriers can tunnel in all energy. The qualitative current-voltage *I-V* characteristic is shown in (e).

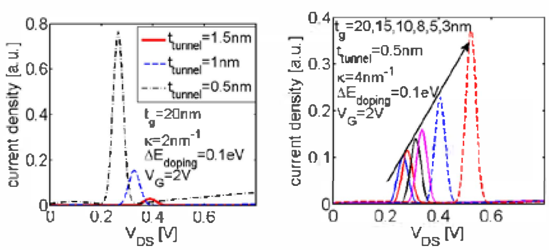

Figure 2: I_D -V_{DS} characteristic with scaling of (a) the tunneling insulator thickness and (b) the gate insulator thickness. The thickness of tunneling insulator strongly affects the tunneling current. Gate control is more effective with thinner t_{gate}. Thus electrostatic doing increase, ΔE increases and peak current increases.

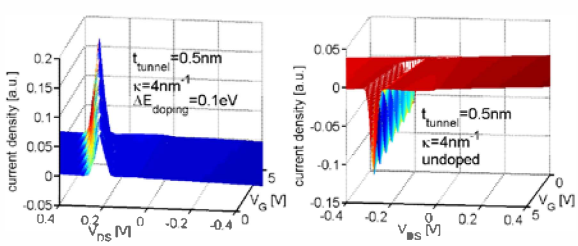

Figure 3: The contour plot of the complete bias space for (a) chemical doping ΔE = 0.1eV and (b) no chemical doping.

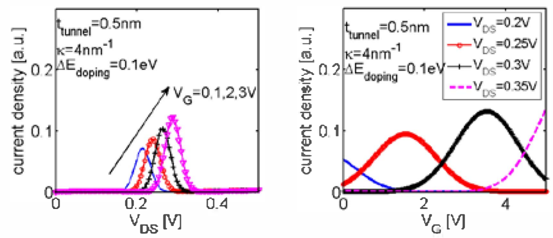

Figure 4: (a) I_D *vs.* V_{DS} curve with different V_G, large V_G induced higher doping effect and increases ΔE. V_{DSp} increases and peak current also increases. (b) I_D *vs.* V_G at different V_{DS}. Transconductance is large in the range where current resonance peak exists.

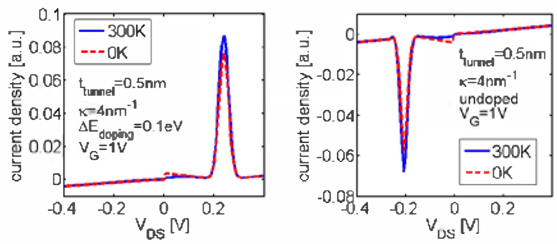

Figure 5: The *I-V* characteristics stay almost the same between T = 300K and T = 0K, since the tunneling current is insensitive to temperature. The difference at low V_{DS}, is due to the Fermi function varying with temperature. The increase of resonant peak current is because Fermi tail extends to high energy with larger density of states.

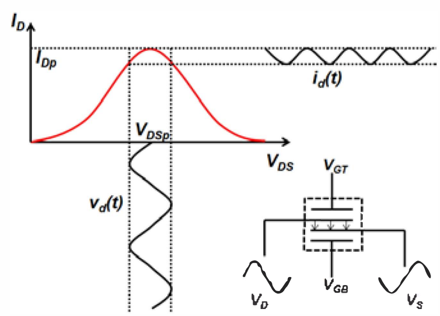

Figure 6: The red curve is the sketch of the symmetric resonance current peak, when V_{DSp} bias at resonance peak with an ac signal. The frequency of the ac signal will be double. The symmetric of conductance band and valence band in graphene offers such behavior.

$$V_{ch1}(V_G,V_D) = -V_{ch2}(V_G,V_D) = V_D + \frac{(2C_t+C_g)\pi(\hbar v_F/q)^2}{4q} - \sqrt{\frac{(2C_t+C_g)\pi(\hbar v_F/q)^2}{2q}V_D - \frac{\pi(\hbar v_F/q)^2}{2q}C_gV_G + \frac{(2C_t+C_g)^2\pi^2(\hbar v_F/q)^4}{16q^2}}$$

$(V_D > 0)$

$$V_{ch1}(V_G,V_D) = -V_{ch2}(V_G,V_D) = V_D - \frac{(2C_t+C_g)\pi(\hbar v_F/q)^2}{4q} + \sqrt{-\frac{(2C_t+C_g)\pi(\hbar v_F/q)^2}{2q}V_D + \frac{\pi(\hbar v_F/q)^2}{2q}C_gV_G + \frac{(2C_t+C_g)^2\pi^2(\hbar v_F/q)^4}{16q^2}}$$

$(V_D < 0)$

Table 1. The equations of channel potential as a function of gates and S/D biases. Since the device is designed to be complete symmetric, $V_{ch1} = -V_{ch2}$.

(This work is supported by the Semiconductor Research Corporation Nanoelectronics Research Initiative and the National Institute of Standards and Technology through the Midwest Institute for Nanoelectronics Discovery (MIND).)